

# New Symmetry Energy Constraint from a Model-Independent Measurement of Isospin Diffusion with INDRA-FAZIA

Caterina Ciampi



*for the INDRA-FAZIA collaboration*

GANIL seminar

*June 24th, 2025*

# Outline

Final results of the E789 experiment

## ① Introduction

- Nuclear equation of state
- Isospin transport phenomena

## ② Experimental data

- The INDRA-FAZIA apparatus
- Model-independent impact parameter reconstruction
- Isospin analysis

## ③ Model predictions and comparison

- BUU@VECC-McGill simulations
- Comparison protocol
- Extraction of the sensitive density
- Constraint on the symmetry energy

# Isospin transport phenomena

Probing the symmetry energy of the nEoS

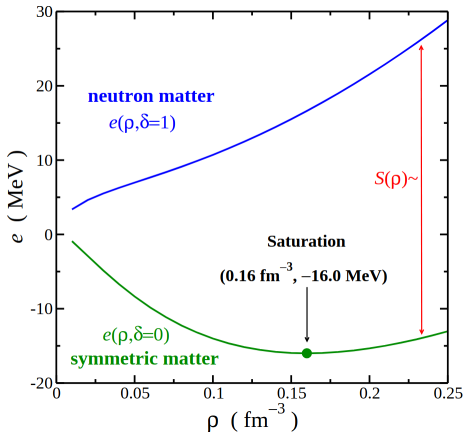
**Nuclear Equation of State (nEoS):** Thermodynamic description of nuclear matter.

# Isospin transport phenomena

Probing the symmetry energy of the nEoS

**Nuclear Equation of State (nEoS):** Thermodynamic description of nuclear matter.

$$e(\rho, \delta) = e(\rho) + S(\rho)\delta^2 \rightarrow \text{Largest uncertainties on symmetry energy } S(\rho)$$

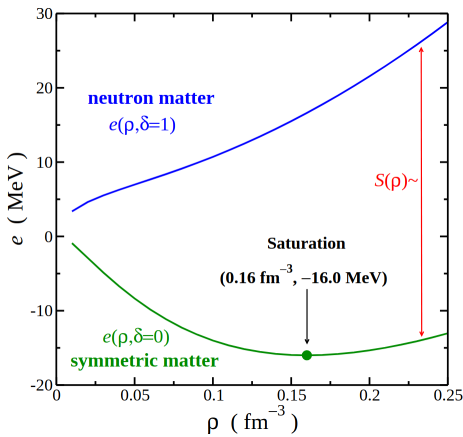


# Isospin transport phenomena

Probing the symmetry energy of the nEoS

**Nuclear Equation of State (nEoS):** Thermodynamic description of nuclear matter.

$$e(\rho, \delta) = e(\rho) + S(\rho)\delta^2 \rightarrow \text{Largest uncertainties on symmetry energy } S(\rho)$$



**Isospin transport phenomena:**  
sensitive probe to study  $S(\rho)$

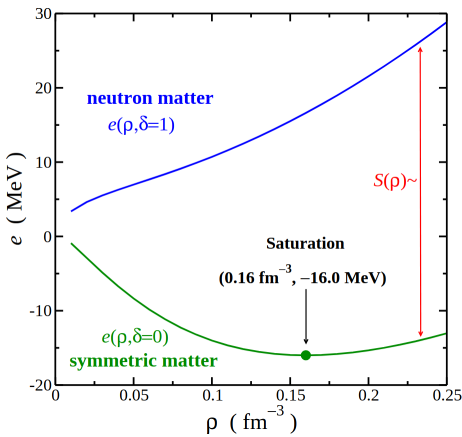
$$\mathbf{j}_n - \mathbf{j}_p \propto S(\rho) \nabla \delta + \delta \frac{\partial S(\rho)}{\partial \rho} \nabla \rho$$

# Isospin transport phenomena

Probing the symmetry energy of the nEoS

**Nuclear Equation of State (nEoS):** Thermodynamic description of nuclear matter.

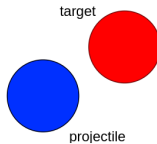
$$e(\rho, \delta) = e(\rho) + S(\rho)\delta^2 \rightarrow \text{Largest uncertainties on symmetry energy } S(\rho)$$



**Isospin transport phenomena:**  
sensitive probe to study  $S(\rho)$

$$\mathbf{j}_n - \mathbf{j}_p \propto \boxed{S(\rho)} \nabla \delta + \delta \frac{\partial S(\rho)}{\partial \rho} \nabla \rho$$

*Isospin diffusion:* driven by isospin gradient in the system, leads to isospin equilibration.

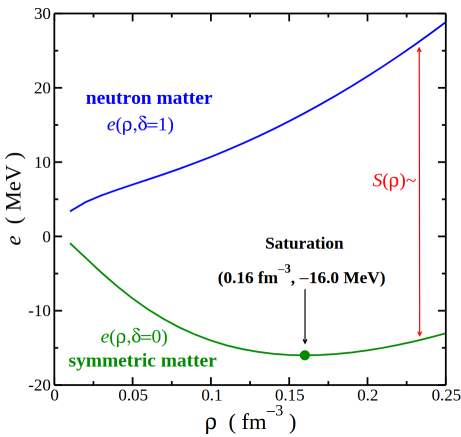


# Isospin transport phenomena

Probing the symmetry energy of the nEoS

**Nuclear Equation of State (nEoS):** Thermodynamic description of nuclear matter.

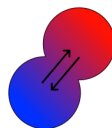
$$e(\rho, \delta) = e(\rho) + S(\rho)\delta^2 \rightarrow \text{Largest uncertainties on symmetry energy } S(\rho)$$



**Isospin transport phenomena:**  
sensitive probe to study  $S(\rho)$

$$\mathbf{j}_n - \mathbf{j}_p \propto \boxed{S(\rho)} \nabla \delta + \delta \frac{\partial S(\rho)}{\partial \rho} \nabla \rho$$

*Isospin diffusion:* driven by isospin gradient in the system, leads to isospin equilibration.

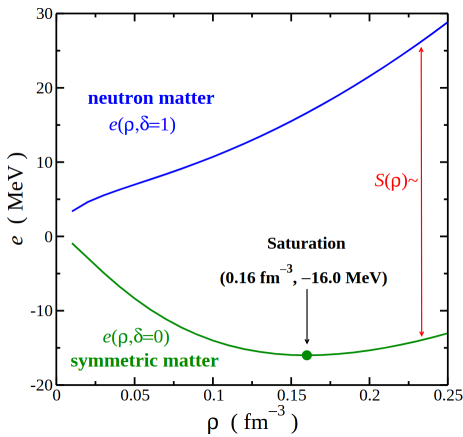


# Isospin transport phenomena

Probing the symmetry energy of the nEoS

**Nuclear Equation of State (nEoS):** Thermodynamic description of nuclear matter.

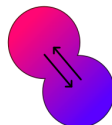
$$e(\rho, \delta) = e(\rho) + S(\rho)\delta^2 \rightarrow \text{Largest uncertainties on symmetry energy } S(\rho)$$



**Isospin transport phenomena:**  
sensitive probe to study  $S(\rho)$

$$\mathbf{j}_n - \mathbf{j}_p \propto \boxed{S(\rho)} \nabla \delta + \delta \frac{\partial S(\rho)}{\partial \rho} \nabla \rho$$

*Isospin diffusion:* driven by isospin gradient in the system, leads to isospin equilibration.

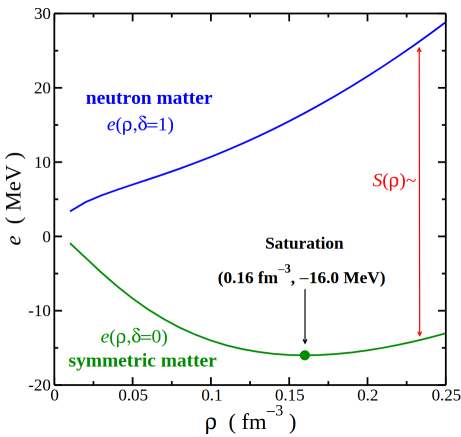


# Isospin transport phenomena

Probing the symmetry energy of the nEoS

**Nuclear Equation of State (nEoS):** Thermodynamic description of nuclear matter.

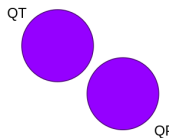
$$e(\rho, \delta) = e(\rho) + S(\rho)\delta^2 \rightarrow \text{Largest uncertainties on symmetry energy } S(\rho)$$



**Isospin transport phenomena:**  
sensitive probe to study  $S(\rho)$

$$\mathbf{j}_n - \mathbf{j}_p \propto \boxed{S(\rho)} \nabla \delta + \delta \frac{\partial S(\rho)}{\partial \rho} \nabla \rho$$

*Isospin diffusion:* driven by isospin gradient in the system, leads to isospin equilibration.



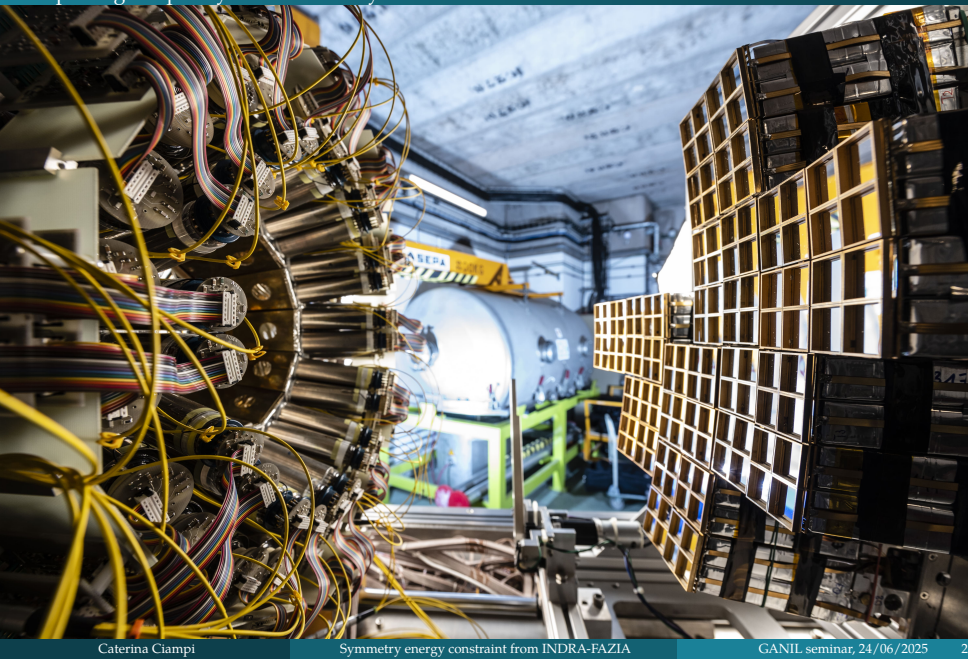
# Experimental data

*or*

*what do we need to “measure” isospin diffusion?*

# The INDRA-FAZIA setup

Exploring isospin dynamics in heavy ion collisions



# The INDRA-FAZIA setup

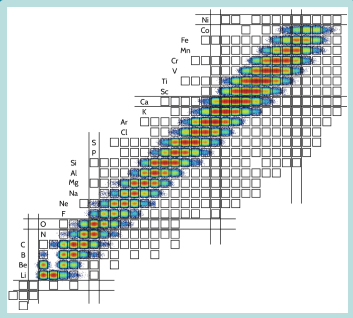
Exploring isospin dynamics in heavy ion collisions

## FAZIA

*Forward-angle A and Z Identification Array*

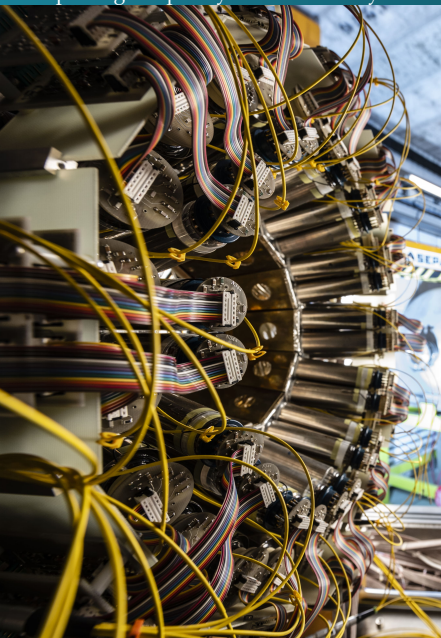
State of the art of ion identification  
in the Fermi energy domain

Covers the most forward polar angles  
for ( $Z, A$ ) identification of QP-like fragments



# The INDRA-FAZIA setup

Exploring isospin dynamics in heavy ion collisions



## INDRA

*Identification de Noyaux et Détection  
avec Résolutions Accrues*



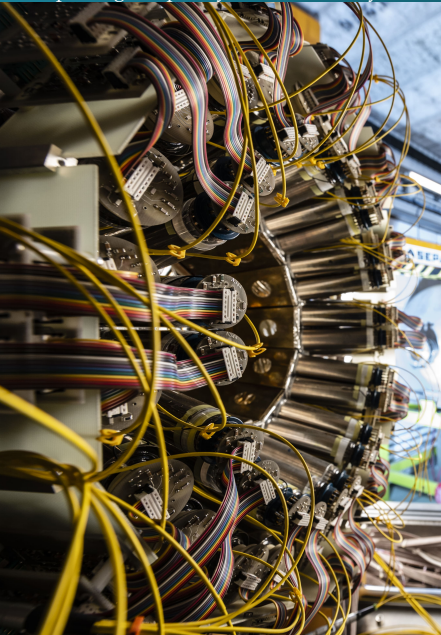
Offers large solid angle coverage  
(~80% of  $4\pi$ ) with high granularity

Provides a good  
global event reconstruction

Build global variables for  
reaction centrality estimation

# The INDRA-FAZIA setup

Exploring isospin dynamics in heavy ion collisions



## INDRA

*Identification de Noyaux et Détection  
avec Résolutions Accrues*



Offers large solid angle coverage  
(~80% of  $4\pi$ ) with high granularity

Provides a good  
global event reconstruction

Build global variables for  
reaction centrality estimation

# Impact parameter reconstruction

Basic structure of the method

Centrality-related observable  $X \longleftrightarrow$  deduce the correspondence with  $b$   
(see J. D. Frankland et al., PRC104, 034609 (2021), R. Rogly et al., PRC98, 024902 (2018))  
⇒ Need to model the conditional probability distribution:  $P(X|b)$

## Step 1

Parametrize the  $P(X|b)$ ,  
taking into account both  
the mean value and the  
fluctuations

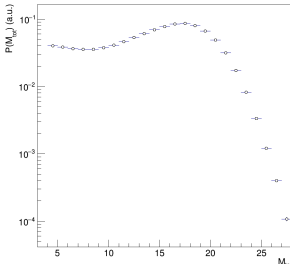
# Impact parameter reconstruction

Basic structure of the method

Centrality-related observable  $X \longleftrightarrow$  deduce the correspondence with  $b$   
(see J. D. Frankland et al., PRC104, 034609 (2021), R. Rogly et al., PRC98, 024902 (2018))  
⇒ Need to model the conditional probability distribution:  $P(X|b)$

## Step 1

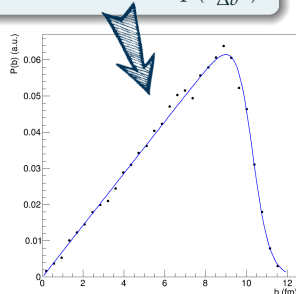
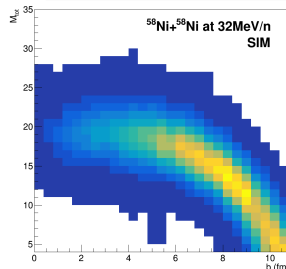
Parametrize the  $P(X|b)$ , taking into account both the mean value and the fluctuations



## Step 2

From the **inclusive** distribution  $P(X)$ , extract the  $P(X|b)$  parameters by fitting:

$$P(X) = \int_0^{\infty} P(b) P(X|b) db \quad P(b) = \frac{2\pi b}{1 + \exp\left(\frac{b - b_0}{\Delta b}\right)}$$



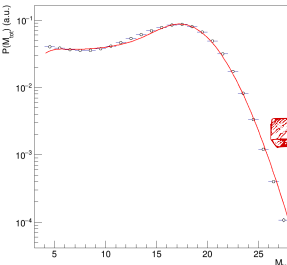
# Impact parameter reconstruction

Basic structure of the method

Centrality-related observable  $X \longleftrightarrow$  deduce the correspondence with  $b$   
(see J. D. Frankland et al., PRC104, 034609 (2021), R. Rogly et al., PRC98, 024902 (2018))  
⇒ Need to model the conditional probability distribution:  $P(X|b)$

## Step 1

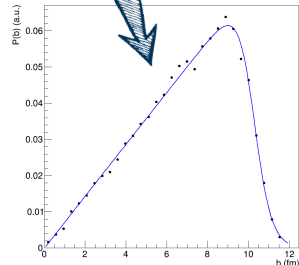
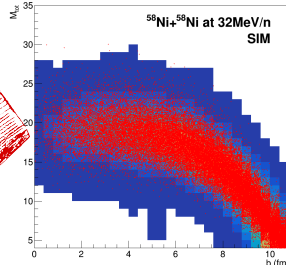
Parametrize the  $P(X|b)$ , taking into account both the mean value and the fluctuations



## Step 2

From the **inclusive** distribution  $P(X)$ , extract the  $P(X|b)$  parameters by fitting:

$$P(X) = \int_0^{\infty} P(b) P(X|b) db \quad P(b) = \frac{2\pi b}{1 + \exp\left(\frac{b - b_0}{\Delta b}\right)}$$



# Impact parameter reconstruction

Basic structure of the method

Centrality-related observable  $X \longleftrightarrow$  deduce the correspondence with  $b$

(see J. D. Frankland et al., PRC104, 034609 (2021), R. Rogly et al., PRC98, 024902 (2018))

⇒ Need to model the conditional probability distribution:  $P(X|b)$

## Step 1

Parametrize the  $P(X|b)$ , taking into account both the mean value and the fluctuations

## Step 2

From the **inclusive** distribution  $P(X)$ , extract the  $P(X|b)$  parameters by fitting:

$$P(X) = \int_0^\infty P(b) P(X|b) db \quad P(b) = \frac{2\pi b}{1 + \exp(\frac{b-b_0}{\Delta b})}$$

## Step 3

Having the  $P(X|b)$ , for each  $X$  selection we can evaluate:

$$P(b|x_1 < X < x_2) = \frac{\int_{x_1}^{x_2} P(b, X) dX}{\int_{x_1}^{x_2} P(X) dX} = \frac{\int_{x_1}^{x_2} P(X) P(b|X) dX}{\int_{x_1}^{x_2} P(X) dX} = \frac{\int_{x_1}^{x_2} P(b) P(X|b) dX}{\int_{x_1}^{x_2} P(X) dX}$$



To obtain the impact parameter distribution, it is necessary to perform the fit on the most inclusive  $P(X)$  distribution, for which the  $P(b)$  above can be assumed.

# Impact parameter reconstruction

Applying the method: overview of the INDRA and FAZIA datasets

Here we present a combined analysis of two datasets of Ni-Ni collisions at 32 MeV/nucleon bearing complementary information:

# Impact parameter reconstruction

Applying the method: overview of the INDRA and FAZIA datasets

Here we present a combined analysis of two datasets of Ni-Ni collisions at 32 MeV/nucleon bearing complementary information:

**INDRA-FAZIA dataset** →  $^{58,64}\text{Ni} + ^{58,64}\text{Ni}$  at 32 MeV/nucl.

Includes the information on the *isospin content of the QP remnant*.

Exp. aimed to study the **isospin diffusion mechanism** by comparing the products of the two asymmetric reactions with both the n-rich and n-deficient symmetric systems

# Impact parameter reconstruction

Applying the method: overview of the INDRA and FAZIA datasets

Here we present a combined analysis of two datasets of Ni-Ni collisions at 32 MeV/nucleon bearing complementary information:

**INDRA-FAZIA dataset** →  $^{58,64}\text{Ni} + ^{58,64}\text{Ni}$  at 32 MeV/nucl.

Includes the information on the *isospin content of the QP remnant*.

Exp. aimed to study the **isospin diffusion mechanism** by comparing the products of the two asymmetric reactions with both the n-rich and n-deficient symmetric systems

- Trigger condition:  $M_{\text{FAZIA}} \geq 1$

Some events are discarded in a non-trivial way, especially for semiperipheral collisions.  
The triangular  $P(b)$  distribution does not well represent the experimental one.

# Impact parameter reconstruction

Applying the method: overview of the INDRA and FAZIA datasets

Here we present a combined analysis of two datasets of Ni-Ni collisions at 32 MeV/nucleon bearing complementary information:

**INDRA-FAZIA dataset** →  $^{58,64}\text{Ni} + ^{58,64}\text{Ni}$  at 32 MeV/nuc.

Includes the information on the *isospin content of the QP remnant*.

Exp. aimed to study the **isospin diffusion mechanism** by comparing the products of the two asymmetric reactions with both the n-rich and n-deficient symmetric systems

- Trigger condition:  $M_{\text{FAZIA}} \geq 1$

Some events are discarded in a non-trivial way, especially for semiperipheral collisions.  
The triangular  $P(b)$  distribution does not well represent the experimental one.

**INDRA dataset** →  $^{58}\text{Ni} + ^{58}\text{Ni}$  at 32 MeV/nuc.

- Trigger condition:  $M_{\text{tot}} \geq 4$

Minimum bias, the  $P(b)$  can be well approximated as shown before (with  $\Delta b \approx 0.4\text{fm}$ ).  
(see J. D. Frankland et al., Phys. Rev. C 104, 034609 (2021), E. Vient et al., Phys. Rev. C 98, 044612 (2018))

Suitable for the application of the *impact parameter reconstruction method*.

# Impact parameter reconstruction

Implementation of the impact parameter reconstruction

Procedure for the reaction in common  $^{58}\text{Ni} + ^{58}\text{Ni}$  at 32 MeV/nucl.:

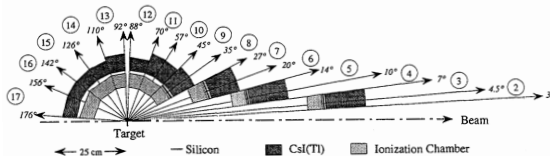
- ① Centrality estimation on “unbiased” INDRA dataset
- ② Apply  $X - b$  relationship to INDRA-FAZIA dataset

# Impact parameter reconstruction

Implementation of the impact parameter reconstruction

Procedure for the reaction in common  $^{58}\text{Ni} + ^{58}\text{Ni}$  at 32 MeV/nucl.:

- ① Centrality estimation on “unbiased” INDRA dataset
- ② Apply  $X - b$  relationship to INDRA-FAZIA dataset

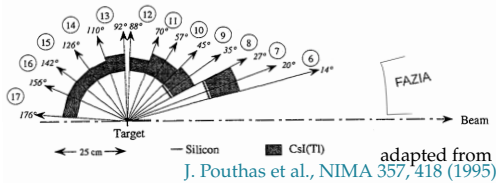


# Impact parameter reconstruction

Implementation of the impact parameter reconstruction

Procedure for the reaction in common  $^{58}\text{Ni} + ^{58}\text{Ni}$  at 32 MeV/nucl.:

- ① Centrality estimation on “unbiased” INDRA dataset
- ② Apply  $X - b$  relationship to INDRA-FAZIA dataset

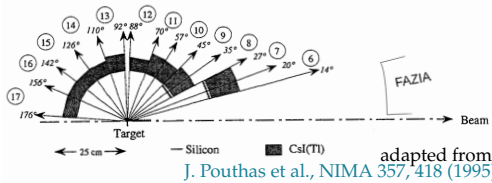


# Impact parameter reconstruction

Implementation of the impact parameter reconstruction

Procedure for the reaction in common  $^{58}\text{Ni} + ^{58}\text{Ni}$  at 32 MeV/nucl.:

- ① Centrality estimation on “unbiased” INDRA dataset
- ② Apply  $X - b$  relationship to INDRA-FAZIA dataset



## Centrality observable X

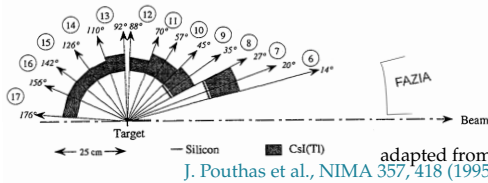
multiplicity  $M$  of *identified* and *unidentified* particles in INDRA rings 6 to 17.

# Impact parameter reconstruction

Implementation of the impact parameter reconstruction

Procedure for the reaction in common  $^{58}\text{Ni} + ^{58}\text{Ni}$  at 32 MeV/nucl.:

- ① Centrality estimation on “unbiased” INDRA dataset
- ② Apply  $X - b$  relationship to INDRA-FAZIA dataset



## Centrality observable X

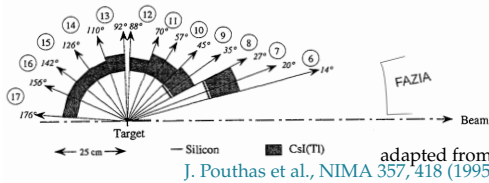
multiplicity  $M$  of *identified* and *unidentified* particles in INDRA rings 6 to 17.

# Impact parameter reconstruction

Implementation of the impact parameter reconstruction

Procedure for the reaction in common  $^{58}\text{Ni} + ^{58}\text{Ni}$  at 32 MeV/nucl.:

- ① Centrality estimation on “unbiased” INDRA dataset
- ② Apply  $X - b$  relationship to INDRA-FAZIA dataset



## Centrality observable X

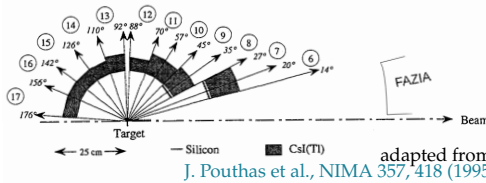
multiplicity  $M$  of *identified* and *unidentified* particles in INDRA rings 6 to 17.

# Impact parameter reconstruction

Implementation of the impact parameter reconstruction

Procedure for the reaction in common  $^{58}\text{Ni} + ^{58}\text{Ni}$  at 32 MeV/nucl.:

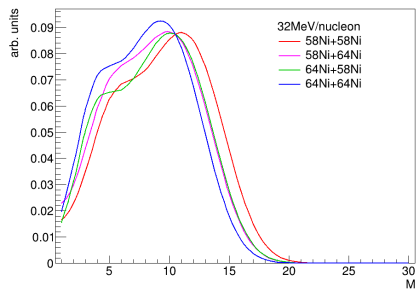
- ① Centrality estimation on “unbiased” INDRA dataset
- ② Apply  $X - b$  relationship to INDRA-FAZIA dataset



## Centrality observable X

multiplicity  $M$  of *identified* and *unidentified* particles in INDRA rings 6 to 17.

Procedure for the other systems:

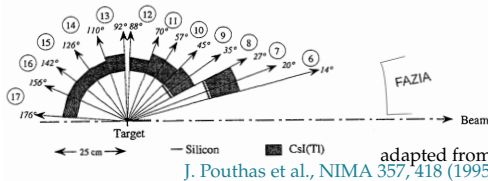


# Impact parameter reconstruction

Implementation of the impact parameter reconstruction

Procedure for the reaction in common  $^{58}\text{Ni} + ^{58}\text{Ni}$  at 32 MeV/nucl.:

- 1 Centrality estimation on “unbiased” INDRA dataset
- 2 Apply  $X - b$  relationship to INDRA-FAZIA dataset



## Centrality observable X

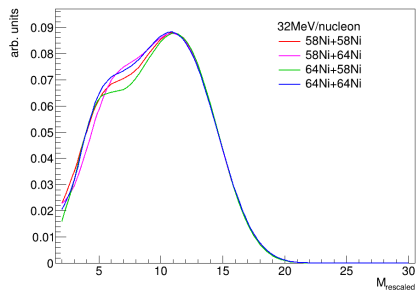
multiplicity  $M$  of *identified* and *unidentified* particles in INDRA rings 6 to 17.

Procedure for the other systems:

→ rescale the detected multiplicity  $M_{\text{sys}}$  into a corresponding  $M_{\text{resc}}$  value for  $^{58}\text{Ni} + ^{58}\text{Ni}$ .

$$M_{\text{resc}} = \lfloor \alpha \cdot (M_{\text{sys}} + r) + \beta \rfloor$$

where  $r \sim U([0, 1])$  is a uniformly distributed random variable taking values in  $[0, 1]$ .



# Impact parameter reconstruction

Setting the parameters for  $P(b)$  model independently

To set the parameters of  $P(b)$  in a model independent way:

$$P(b) = \frac{2\pi b}{1 + \exp[(b - b_0)/\Delta b]}$$

$\Delta b \approx 0.4 \text{ fm}$  as verified in PRC 104, 034609 (2021)

$b_0$  by inverting  $\sigma_R = -2\pi(\Delta b)^2 \text{Li}_2\left[-\exp\left(\frac{b_0}{\Delta b}\right)\right]$

# Impact parameter reconstruction

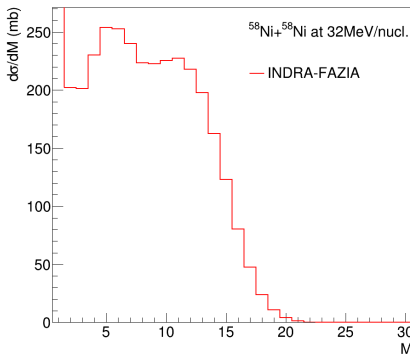
Setting the parameters for  $P(b)$  model independently

To set the parameters of  $P(b)$  in a model independent way:

$$P(b) = \frac{2\pi b}{1 + \exp[(b - b_0)/\Delta b]}$$

$\Delta b \approx 0.4 \text{ fm}$  as verified in PRC 104, 034609 (2021)

$b_0$  by inverting  $\sigma_R = -2\pi(\Delta b)^2 \text{Li}_2\left[-\exp\left(\frac{b_0}{\Delta b}\right)\right]$



For the estimation of  $\sigma_R$ , and hence  $b_0$ :

- Use the elastic scattering events in the INDRA-FAZIA dataset ( $M_{FAZIA} \geq 1$ ) as reference for cross section normalization

# Impact parameter reconstruction

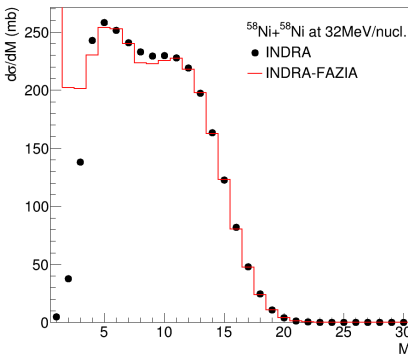
Setting the parameters for  $P(b)$  model independently

To set the parameters of  $P(b)$  in a model independent way:

$$P(b) = \frac{2\pi b}{1 + \exp[(b - b_0)/\Delta b]}$$

$\Delta b \approx 0.4 \text{ fm}$  as verified in PRC 104, 034609 (2021)

$b_0$  by inverting  $\sigma_R = -2\pi(\Delta b)^2 \text{Li}_2\left[-\exp\left(\frac{b_0}{\Delta b}\right)\right]$



For the estimation of  $\sigma_R$ , and hence  $b_0$ :

- Use the elastic scattering events in the INDRA-FAZIA dataset ( $M_{FAZIA} \geq 1$ ) as reference for cross section normalization
- Transfer the normalization to the INDRA dataset using the high multiplicity tail, after correcting for small trigger effect

# Impact parameter reconstruction

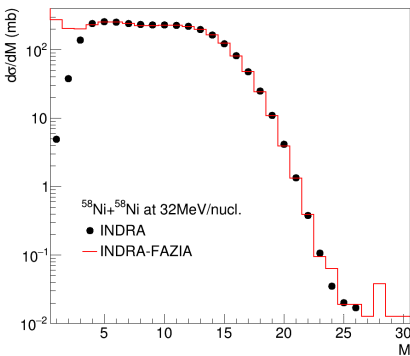
Setting the parameters for  $P(b)$  model independently

To set the parameters of  $P(b)$  in a model independent way:

$$P(b) = \frac{2\pi b}{1 + \exp[(b - b_0)/\Delta b]}$$

$\Delta b \approx 0.4 \text{ fm}$  as verified in PRC 104, 034609 (2021)

$b_0$  by inverting  $\sigma_R = -2\pi(\Delta b)^2 \text{Li}_2\left[-\exp\left(\frac{b_0}{\Delta b}\right)\right]$

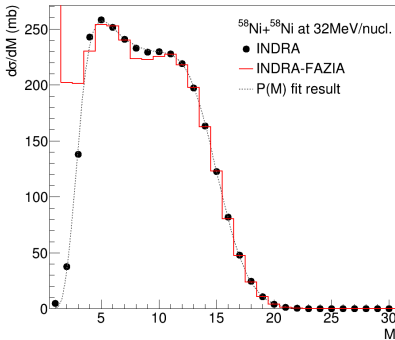


For the estimation of  $\sigma_R$ , and hence  $b_0$ :

- Use the elastic scattering events in the INDRA-FAZIA dataset ( $M_{\text{FAZIA}} \geq 1$ ) as reference for cross section normalization
- Transfer the normalization to the INDRA dataset using the high multiplicity tail, after correcting for small trigger effect
- From the total reaction cross section  $\sigma_R$  for INDRA dataset  $\Rightarrow b_0 = (9.8 \pm 0.7) \text{ fm}$

# Impact parameter reconstruction

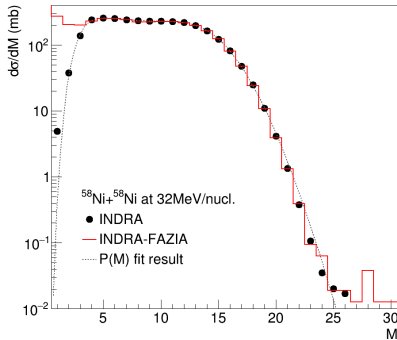
Results of the method



Fit result on multiplicity  $M$  of identified and unidentified particles in INDRA rings 6-17 for  $^{58}\text{Ni} + ^{58}\text{Ni}$  at 32 MeV/nucleon on INDRA dataset

# Impact parameter reconstruction

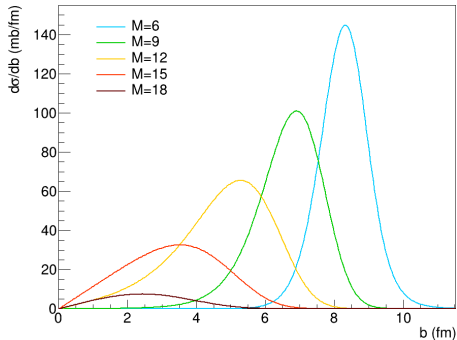
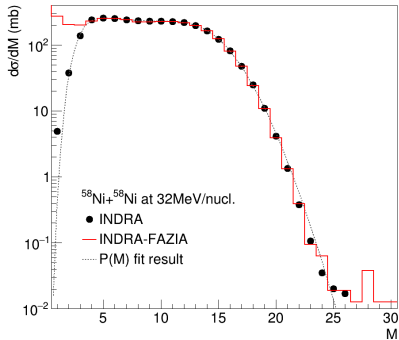
Results of the method



Fit result on multiplicity  $M$  of identified and unidentified particles in INDRA rings 6-17 for  $^{58}\text{Ni} + ^{58}\text{Ni}$  at 32 MeV/nucleon on INDRA dataset

# Impact parameter reconstruction

Results of the method



Fit result on multiplicity  $M$  of identified and unidentified particles in INDRA rings 6-17 for  $^{58}\text{Ni} + ^{58}\text{Ni}$  at 32 MeV/nucleon on INDRA dataset

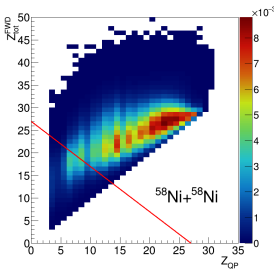
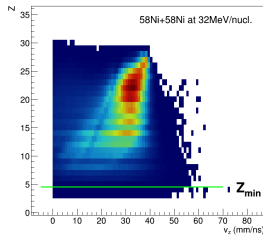
→ important role of **intrinsic fluctuations**: relatively different  $M$  selections populate partly (or entirely) superimposed  $b$  intervals

# Isospin analysis

## Selection of the events

In view of producing the most general result, easily comparable with any theoretical prediction, we avoid a strictly exclusive analysis.

- No distinction among different output channels
- QP remnant selected as:
  - ➊ fragment with largest  $Z$  in forward hemisphere
  - ➋ if more than one with same  $Z$ , select largest  $v_z^{\text{c.m.}}$
- Minimum size to consider a QP remnant:  $Z_{QP} \geq 5$   
→ include light products from very dissipative events



Carefully check the completeness of the event:

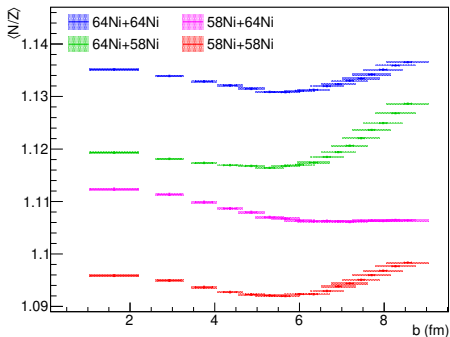
- The total undetected charge in the forward hemisphere should not exceed  $Z_{QP}$
- Accept event if  $Z_{QP} \geq 28 - Z_{\text{tot}}^{\text{FWD}}$
- We verified that by removing < 13% of events, the final result becomes stable against reasonable variations of  $Z_{QP}^{\text{min}}$

# Isospin analysis

## Evolution of isospin equilibration with centrality

Each event is assigned an impact parameter value randomly drawn from the  $b$  distribution associated with its corresponding  $M_{\text{rec}}$ .

⇒ Take into account the fluctuations



**Model-independent  $\langle N/Z \rangle$  for the QP remnant as a function of  $b$  for the four systems in the INDRA-FAZIA dataset**

Clear effect of isospin equilibration down to the most central collisions:

- *peripheral*: similar result for reactions with same projectile
- *central*:  $\langle N/Z \rangle$  depends on target, mixed systems tend to each other

The horizontal error bars are associated with the uncertainty on the estimation of  $b_0$  in the  $P(b)$  assumed for the impact parameter reconstruction method, affecting less central collisions to a greater extent.

# Isospin analysis

Model independent isospin transport ratio

**Isospin transport ratio:** can highlight the isospin diffusion effect, bypassing the effects acting similarly on the four systems ([F. Rami et al., Phys. Rev. Lett. 84, 1120 \(2000\)](#))

$$R(x) = \frac{2x_i - x_{AA} - x_{BB}}{x_{AA} - x_{BB}}$$

where  $x$  is an isospin sensitive observable,  
 $A = {}^{64}\text{Ni}$ ,  $B = {}^{58}\text{Ni}$  and  $i = AA, AB, BA, BB$ .

# Isospin analysis

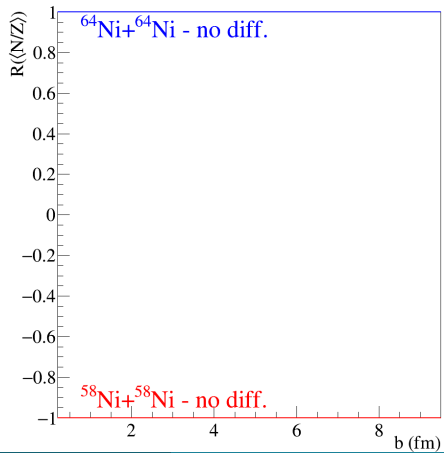
Model independent isospin transport ratio

**Isospin transport ratio:** can highlight the isospin diffusion effect, bypassing the effects acting similarly on the four systems (F. Rami et al., Phys. Rev. Lett. 84, 1120 (2000))

$$R(x) = \frac{2x_i - x_{AA} - x_{BB}}{x_{AA} - x_{BB}}$$

$R(x) = \pm 1 \rightarrow$  non equilibrated

where  $x$  is an isospin sensitive observable,  
 $A = {}^{64}\text{Ni}$ ,  $B = {}^{58}\text{Ni}$  and  $i = \textcolor{blue}{AA}, \textcolor{blue}{AB}, \textcolor{red}{BA}, \textcolor{red}{BB}$ .



# Isospin analysis

Model independent isospin transport ratio

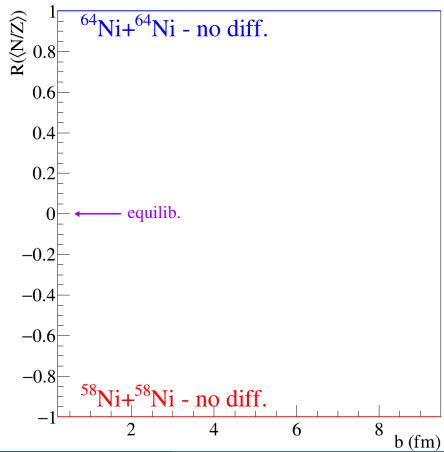
**Isospin transport ratio:** can highlight the isospin diffusion effect, bypassing the effects acting similarly on the four systems (F. Rami et al., Phys. Rev. Lett. 84, 1120 (2000))

$$R(x) = \frac{2x_i - x_{AA} - x_{BB}}{x_{AA} - x_{BB}}$$

$R(x) = \pm 1 \rightarrow \text{non equilibrated}$

$R(x_{AB}) = R(x_{BA}) \rightarrow \text{full equilibration}$

where  $x$  is an isospin sensitive observable,  
 $A = {}^{64}\text{Ni}$ ,  $B = {}^{58}\text{Ni}$  and  $i = AA, AB, BA, BB$ .



# Isospin analysis

Model independent isospin transport ratio

**Isospin transport ratio:** can highlight the isospin diffusion effect, bypassing the effects acting similarly on the four systems (F. Rami et al., Phys. Rev. Lett. 84, 1120 (2000))

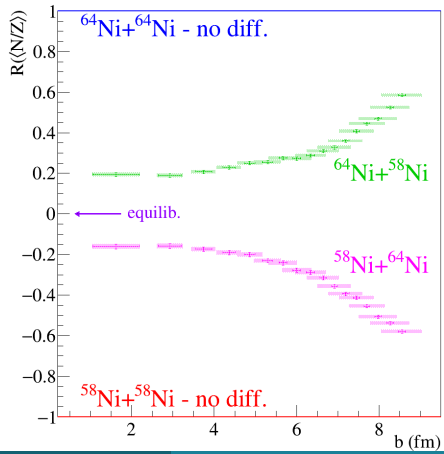
$$R(x) = \frac{2x_i - x_{AA} - x_{BB}}{x_{AA} - x_{BB}}$$

$R(x) = \pm 1 \rightarrow$  non equilibrated

$R(x_{AB}) = R(x_{BA}) \rightarrow$  full equilibration

where  $x$  is an isospin sensitive observable,  
 $A = {}^{64}\text{Ni}$ ,  $B = {}^{58}\text{Ni}$  and  $i = AA, AB, BA, BB$ .

**Model-independent isospin transport ratio**  
 $R(\langle N/Z \rangle)$  for the QP remnant as a function  
of the impact parameter  $b$



# Isospin analysis

Model independent isospin transport ratio

**Isospin transport ratio:** can highlight the isospin diffusion effect, bypassing the effects acting similarly on the four systems (F. Rami et al., Phys. Rev. Lett. 84, 1120 (2000))

$$R(x) = \frac{2x_i - x_{AA} - x_{BB}}{x_{AA} - x_{BB}}$$

$R(x) = \pm 1 \rightarrow$  non equilibrated

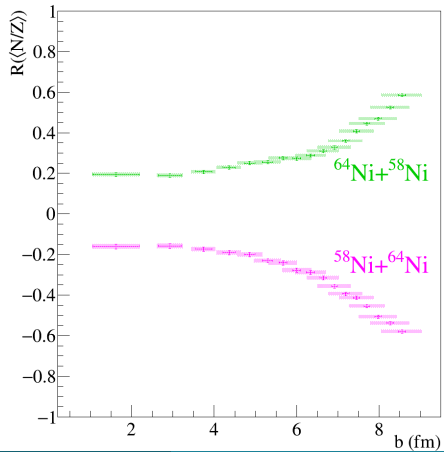
$R(x_{AB}) = R(x_{BA}) \rightarrow$  full equilibration

where  $x$  is an isospin sensitive observable,  
 $A = {}^{64}\text{Ni}$ ,  $B = {}^{58}\text{Ni}$  and  $i = AA, AB, BA, BB$ .

**Model-independent isospin transport ratio  
 $R(\langle N/Z \rangle)$  for the QP remnant as a function  
of the impact parameter  $b$**

Experimental result providing a reference for comparison with theoretical predictions from transport models.

C. Ciampi et al., Phys. Rev. C 111, 044601 (2025)



# Model predictions

*or*

*how do we extract a constraint on the symmetry energy?*

Extract information on  
**symmetry energy term**  
of nuclear EoS

INDRA-FAZIA experimental data

BUU@VECC-McGill calculations

Compare the experimental isospin transport ratio with the one predicted for *primary fragments* by the transport code:

- Avoid spurious effect from afterburner coupling
- Exploit i.t.r. property of largely suppressing the effects of statistical deexcitation  
[A. Camaiani et al., Phys. Rev. C 102, 044607 \(2020\)](#), [S. Mallik et al., J. Phys. G 49, 015102 \(2021\)](#)

Simulations carried out with the BUU@VECC-McGill transport code:

[S. Mallik et al., Phys. Rev. C 91, 034616 \(2015\)](#)

- BUU code, setting 100 test particles/nucleon
- 8 impact parameters for each reaction/parametrization
- 200 events for each impact parameter/reaction/parametrization
- Simulation run until 300fm/c (ITR convergence)
- Possibility to plug in and test different nEoS via metamodeling technique

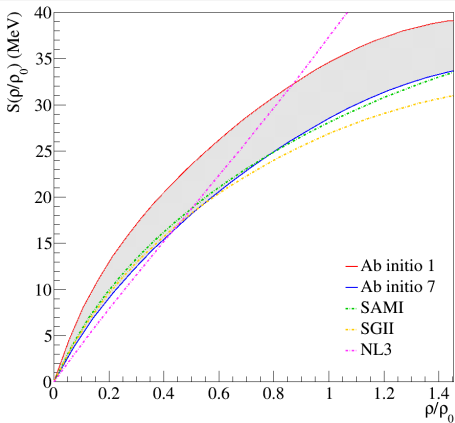
[J. Margueron et al., Phys. Rev. C 97, 025805 \(2018\)](#)

# BUU@VECC-McGill simulations

EoS parametrizations from the literature

NEoS parametrizations from *ab initio* and phenomenological approaches:

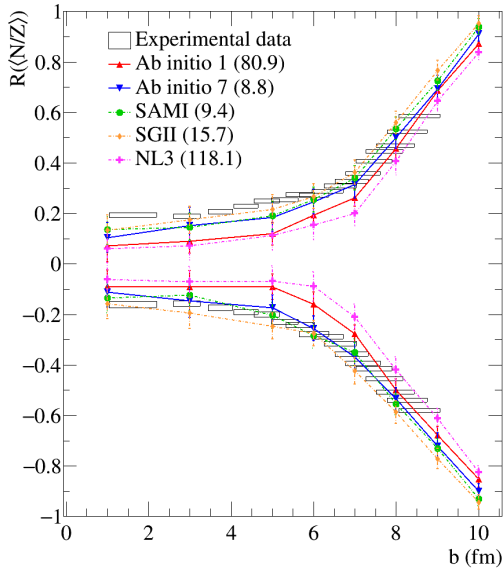
- *Ab initio*: two extreme  $\chi$ -EFT interactions from [C. Drischler et al., Phys. Rev. C 93, 054314 \(2016\)](#)
- Phenomenological approaches:
  - SAMI (Skyrme), [X. Roca-Maza et al., Phys. Rev. C 86, 031306\(R\) \(2012\)](#)
  - SGII (Skyrme), [Nguyen Van Giai et al., Phys. Lett. B106, 379 \(1981\)](#)
  - NL3 (RMF), [G. A. Lalazissis et al., Phys. Rev. C 55, 540 \(1997\)](#)



	$n_{sat}$ (fm $^{-3}$ )	$E_{sat}$ (MeV)	$E_{sym}$ (MeV)	$L_{sym}$ (MeV)	$K_{sat}$ (MeV)	$K_{sym}$ (MeV)
Ab initio 1	0.189	-16.92	34.57	48.5	241	224
Ab initio 7	0.140	-13.23	28.53	43.9	43.9	-144
SAMI	0.1587	-15.93	28.16	43.7	245	-120
SGII	0.1583	-15.59	26.83	37.6	215	-146
NL3	0.1480	-16.24	37.35	118.3	271	101

# BUU@VECC-McGill simulations

Simulated isospin transport ratio



A few observations:

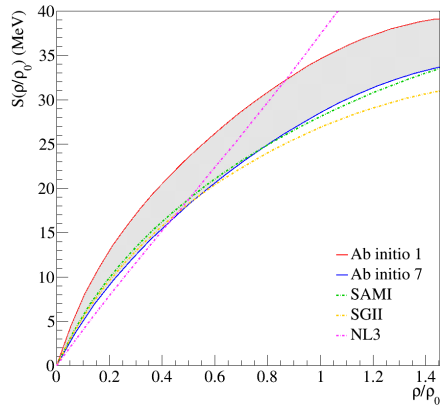
- SAMI vs *ab initio* 7: similar symmetry energy, different isoscalar behavior. Similar ITR indicates we are probing  $E_{sym}$ .
- NL3, *ab initio* 1 → bad match: largest  $E_{sym}$  values above  $0.5\rho_0$  can be excluded.
- SAMI, SGII, *ab initio* 7 → good match: they feature similar  $E_{sym}$  values above  $0.5\rho_0$

$\chi^2$  values calculated by interpolating between the simulated data points:

	AI1	AI7	SAMI	SGII	NL3
$\chi^2$	80.9	8.8	9.4	15.7	118.1

# Experimental-simulated data comparison

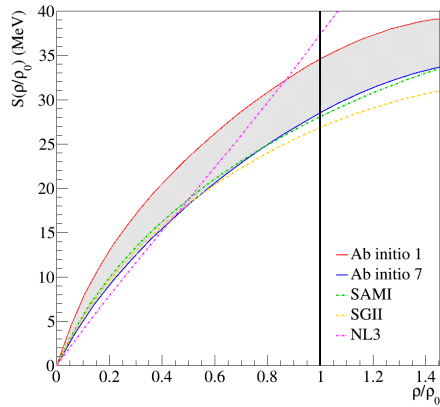
Extraction of approximate confidence regions in the  $S - \rho$  plane



# Experimental-simulated data comparison

Extraction of approximate confidence regions in the  $S - \rho$  plane

At each value of  $\rho/\rho_0$ :

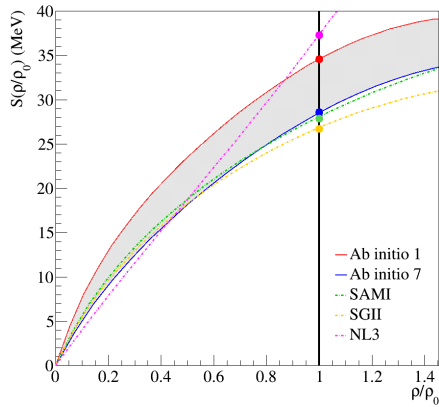


# Experimental-simulated data comparison

Extraction of approximate confidence regions in the  $S - \rho$  plane

At each value of  $\rho/\rho_0$ :

- Pick  $S(\rho/\rho_0)$  values corresponding to the 5 nEoS parametrizations

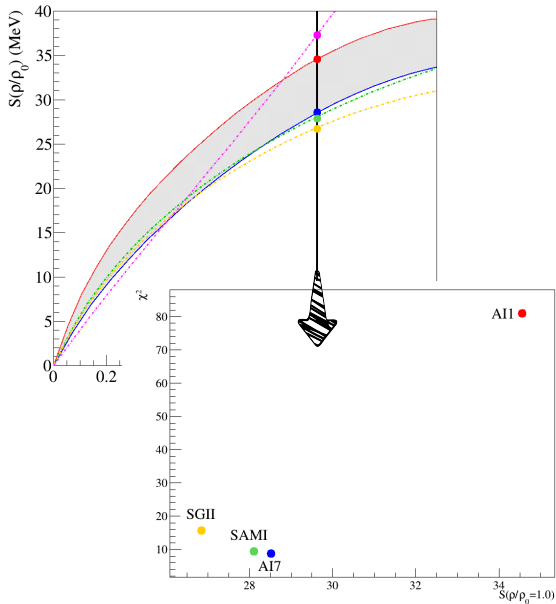


# Experimental-simulated data comparison

Extraction of approximate confidence regions in the  $S - \rho$  plane

At each value of  $\rho/\rho_0$ :

- Pick  $S(\rho/\rho_0)$  values corresponding to the 5 nEoS parametrizations
- Plot the 5  $\chi^2$  values as a function of the  $S(\rho/\rho_0)$  for the corresponding nEoS

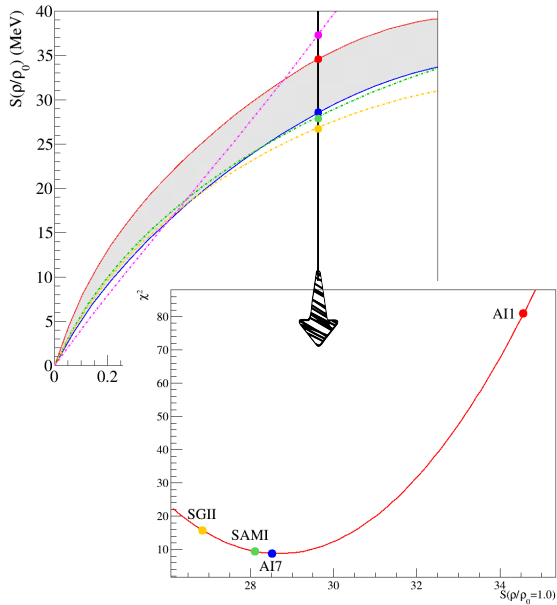


# Experimental-simulated data comparison

Extraction of approximate confidence regions in the  $S - \rho$  plane

At each value of  $\rho/\rho_0$ :

- Pick  $S(\rho/\rho_0)$  values corresponding to the 5 nEoS parametrizations
- Plot the 5  $\chi^2$  values as a function of the  $S(\rho/\rho_0)$  for the corresponding nEoS
- Quadratic fit to extract the parabolic dependence  $\chi^2(S(\rho/\rho_0))$  around its minimum



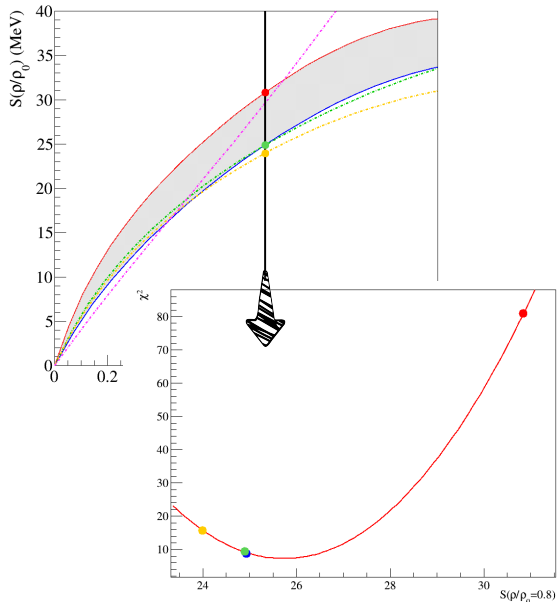
# Experimental-simulated data comparison

Extraction of approximate confidence regions in the  $S - \rho$  plane

At each value of  $\rho/\rho_0$ :

- Pick  $S(\rho/\rho_0)$  values corresponding to the 5 nEoS parametrizations
- Plot the 5  $\chi^2$  values as a function of the  $S(\rho/\rho_0)$  for the corresponding nEoS
- Quadratic fit to extract the parabolic dependence  $\chi^2(S(\rho/\rho_0))$  around its minimum

Repeat along the  $\rho/\rho_0$  axis.



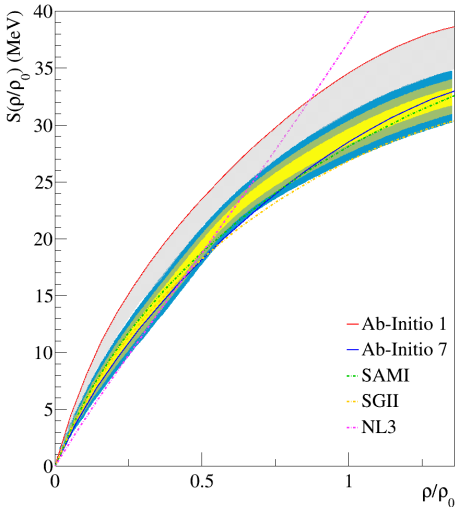
# Experimental-simulated data comparison

## Unweighted confidence regions

At each  $\rho/\rho_0$  we thus define a likelihood along  $S(\rho/\rho_0)$  as:

$$\mathcal{L}(S(\rho/\rho_0)) \propto e^{-\chi^2(S(\rho/\rho_0))/2}$$

- extract the  $N\sigma$  confidence intervals for  $S(\rho/\rho_0)$
- build approximate confidence region in the  $S - \rho/\rho_0$  plane.



# Experimental-simulated data comparison

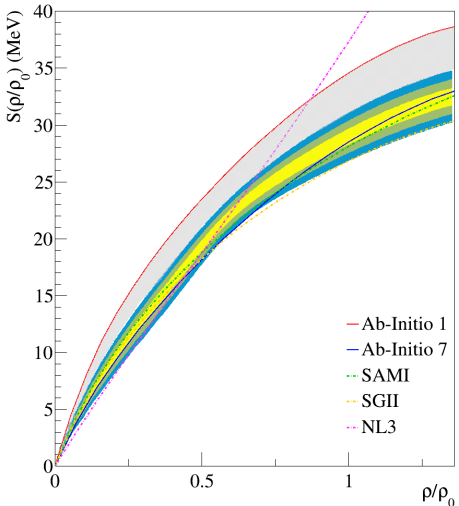
Unweighted confidence regions

At each  $\rho/\rho_0$  we thus define a likelihood along  $S(\rho/\rho_0)$  as:

$$\mathcal{L}(S(\rho/\rho_0)) \propto e^{-\chi^2(S(\rho/\rho_0))/2}$$

- extract the  $N\sigma$  confidence intervals for  $S(\rho/\rho_0)$
- build approximate confidence region in the  $S - \rho/\rho_0$  plane.

For a meaningful constraint we take into account the density region probed by the isospin diffusion phenomenon  
→ define a *weight function*

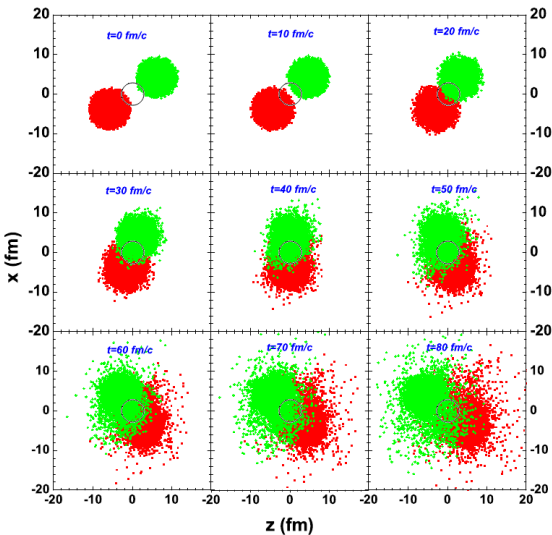


# Sensitive density region

## Isospin diffusion dynamics

Study of the evolution of  
**baryonic density and isospin  
current density** extracted from  
BUU@VECC-McGill

- *Ab initio* 7 nEoS
- 200 events for 4 selected  
impact parameters  
( $b = 3, 5, 7, 9$  fm)
- Quantities evaluated over  
spherical volume with  
 $r = 3$  fm



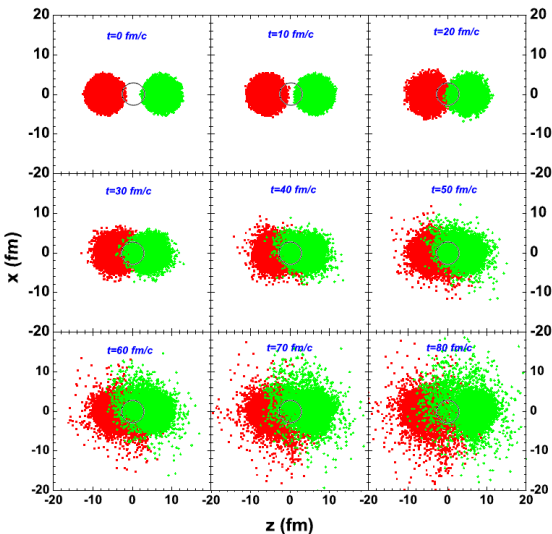
# Sensitive density region

## Isospin diffusion dynamics

Study of the evolution of **baryonic density and isospin current density** extracted from BUU@VECC-McGill

- *Ab initio* 7 nEoS
- 200 events for 4 selected impact parameters ( $b = 3, 5, 7, 9 \text{ fm}$ )
- Quantities evaluated over spherical volume with  $r = 3 \text{ fm}$

Principal axis extracted at each timestep by diagonalizing the momentum of inertia tensor.  
Current densities evaluated in its reference frame.



# Sensitive density region

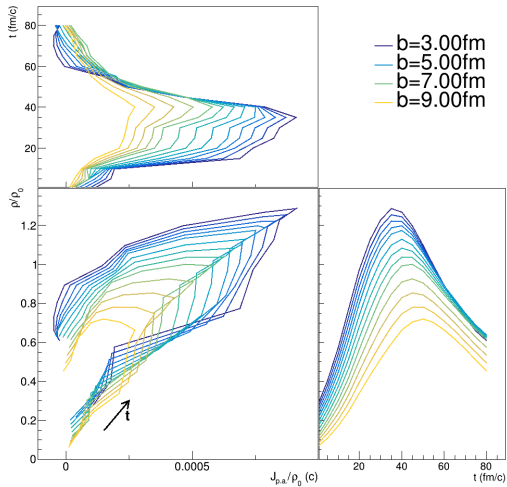
Isospin current and baryonic density

n/p current densities evaluated as:

$$\vec{j}_q^{(X)} = \frac{1}{V} \int_V d^3r \rho_q^{(X)}(\vec{r}) \vec{v}_q^{(X)}(\vec{r}).$$

Nucleon exchange determined by  $\vec{j}_q^{(X)}$  components along the principal axis.

Net isospin current density obtained as the difference between neutron and proton current densities.



# Sensitive density region

Isospin current and baryonic density

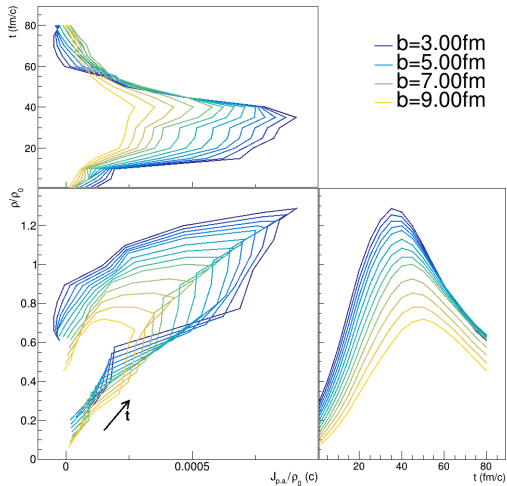
n/p current densities evaluated as:

$$\vec{j}_q^{(X)} = \frac{1}{V} \int_V d^3r \rho_q^{(X)}(\vec{r}) \vec{v}_q^{(X)}(\vec{r}).$$

Nucleon exchange determined by  $\vec{j}_q^{(X)}$  components along the principal axis.

Net isospin current density obtained as the difference between neutron and proton current densities.

**N.B.** maximum exchange found in the compression phase, when the highest densities are reached.



# Sensitive density region

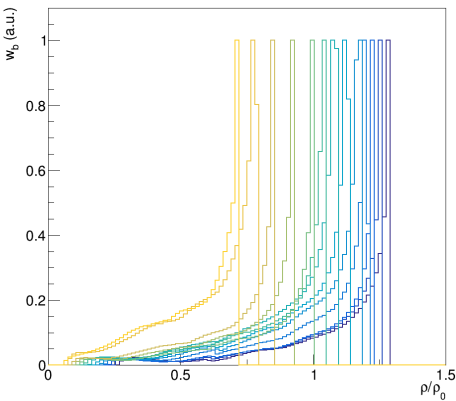
## Weight function

Weight function for a given impact parameter  $w_b(\rho/\rho_0)$ :

built as baryonic density cumulated over time, weighted by the corresponding current density

$$w_b(\rho/\rho_0) = \int_{t_{\text{start}}}^{t_{\text{stop}}} j_{\text{p.a.}}(t) \delta(\rho/\rho_0 - \rho(t)/\rho_0) dt$$

→ evaluated between 0 and 80 fm/c



# Sensitive density region

## Weight function

Weight function for a given impact parameter  $w_b(\rho/\rho_0)$ :

built as baryonic density cumulated over time, weighted by the corresponding current density

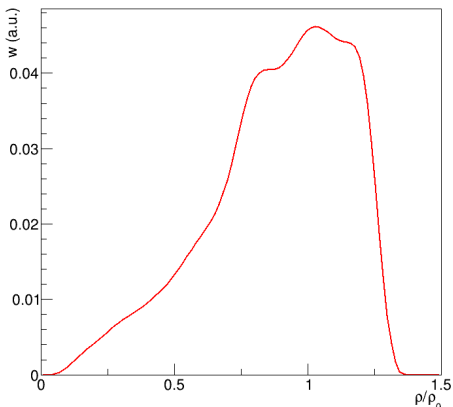
$$w_b(\rho/\rho_0) = \int_{t_{\text{start}}}^{t_{\text{stop}}} j_{\text{p.a.}}(t) \delta(\rho/\rho_0 - \rho(t)/\rho_0) dt$$

→ evaluated between 0 and 80 fm/c

Global weight function  $w(\rho/\rho_0)$ :

$$w(\rho/\rho_0) = \int_{b_{\min}}^{b_{\max}} \tilde{w}_b(\rho/\rho_0) db$$

→  $b$  interval between 3 and 9 fm

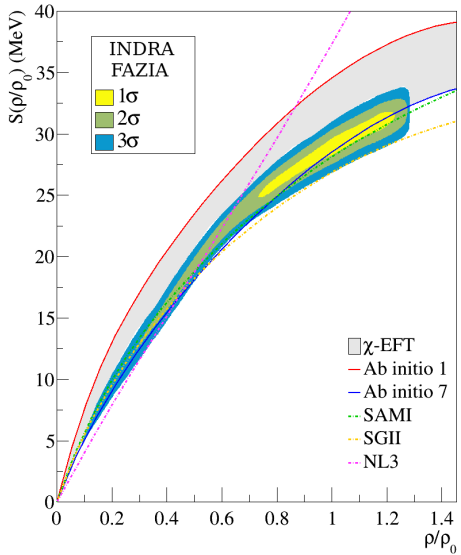


# Constraint on the nuclear EoS

Weighted confidence regions

Confidence regions  $1\sigma, 2\sigma, 3\sigma$  defined based on weighted  $\mathcal{L}(S(\rho/\rho_0))$ :

- Sensitivity close to saturation - anticipated by NL3 rejection, different from SAMI, SGII, AI7 for  $\rho > 0.5\rho_0$



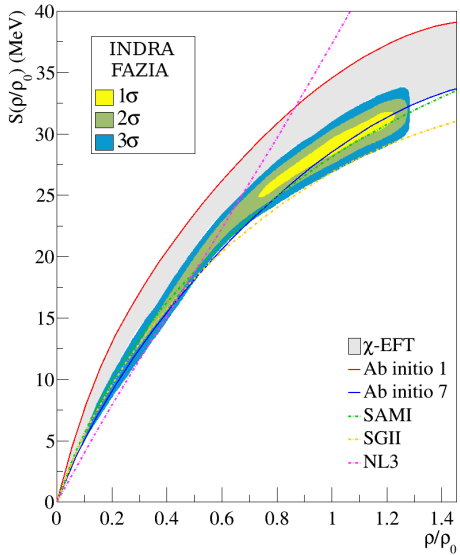
C. Ciampi, S. Mallik *et al.*, submitted (2025).

# Constraint on the nuclear EoS

Weighted confidence regions

Confidence regions  $1\sigma, 2\sigma, 3\sigma$  defined based on weighted  $\mathcal{L}(S(\rho/\rho_0))$ :

- Sensitivity close to saturation - anticipated by NL3 rejection, different from SAMI, SGII, AI7 for  $\rho > 0.5\rho_0$
- Good agreement with  $\chi$ -EFT - towards the softer side of its uncertainty band



C. Ciampi, S. Mallik *et al.*, submitted (2025).

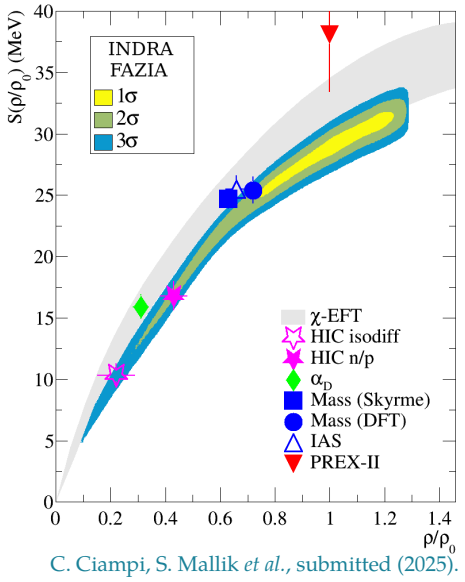
# Constraint on the nuclear EoS

Weighted confidence regions

Confidence regions  $1\sigma, 2\sigma, 3\sigma$  defined based on weighted  $\mathcal{L}(S(\rho/\rho_0))$ :

- Sensitivity close to saturation - anticipated by NL3 rejection, different from SAMI, SGII, AI7 for  $\rho > 0.5\rho_0$
- Good agreement with  $\chi$ -EFT - towards the softer side of its uncertainty band
- Good agreement with isospin diffusion data in Sn+Sn collisions - (but we declare a different  $\rho$  sensitivity)

- W. G. Lynch *et al.*, Phys. Lett. B 830, 137098 (2022).  
M. B. Tsang *et al.*, Phys. Rev. Lett. 102, 122701 (2009).  
P. Morfouace *et al.*, Phys. Lett. B 799, 135045 (2019).  
Z. Zhang *et al.*, Phys. Rev. C 92, 031301R (2015).  
M. Kortelainen *et al.*, Phys. Rev. C 85, 024304 (2012).  
P. Danielewicz *et al.*, Nucl. Phys. A 958, 147 (2017).  
B. T. Reed *et al.*, Phys. Rev. Lett. 126, 172503 (2021).



C. Ciampi, S. Mallik *et al.*, submitted (2025).

# Summary and conclusions

A new nuclear EoS constraint from isospin diffusion data:

- Comparison of model-independent experimentally-measured isospin transport ratio in  $^{58,64}\text{Ni} + ^{58,64}\text{Ni}$  collisions at 32 MeV/nucleon with the predictions of BUU@VECC-McGill transport model.
- EoS from both *ab initio* and phenomenological approaches considered.
- Consistent study of the time dependence of the baryonic density and of the isospin current density for the determination of the density region probed by the experiment.

# Summary and conclusions

A new nuclear EoS constraint from isospin diffusion data:

- Comparison of model-independent experimentally-measured isospin transport ratio in  $^{58,64}\text{Ni} + ^{58,64}\text{Ni}$  collisions at 32 MeV/nucleon with the predictions of BUU@VECC-McGill transport model.
- EoS from both *ab initio* and phenomenological approaches considered.
- Consistent study of the time dependence of the baryonic density and of the isospin current density for the determination of the density region probed by the experiment.

*Thank you!*

C. Ciampi, S. Mallik, F. Gulminelli, D. Gruyer, J. D. Frankland, N. Le Neindre, R. Bougault, A. Chbihi, L. Baldesi, S. Barlini, B. Borderie, A. Camaiani, G. Casini, I. Dekhissi, J. A. Dueñas, Q. Fable, F. Gramegna, M. Henri, B. Hong, S. Kim, A. Kordyasz, T. Kozik, I. Lombardo, O. Lopez, T. Marchi, S. H. Nam, J. Park, M. Pârlig, G. Pasquali, S. Piantelli, G. Poggi, S. Valdré, G. Verde, E. Vient



# *Backup slides*

# Impact parameter reconstruction

Detailed structure of the method

Given a centrality observable  $X$ , its inclusive distribution  $P(X)$  can be expressed as:

$$P(X) = \int_0^\infty P(X, b) db = \int_0^\infty P(b) P(X|b) db = \int_0^1 P(X|c_b) dc_b$$

where a change of variables is applied, introducing the centrality  $c_b \equiv \int_0^b P(b') db'$  and exploiting that  $P(c_b) = 1$ .

**Key step:** model the  $P(X|c_b)$  and extract its parameters by fitting the experimental  $P(X)$ .  $X$  assumes positive values  $\rightarrow$  non-negative gamma distribution as fluctuation kernel:

$$P(X|c_b) = \frac{1}{\Gamma(k)\theta^k} X^{k-1} e^{-X/\theta} \quad \text{where } \bar{X} = k\theta \text{ and } \sigma_X = \sqrt{k}\theta$$

where  $k$  and  $\theta$  generally evolve with centrality. For them we assume:

- $k(c_b) = k_{\max}[1 - c_b^\alpha]^\gamma + k_{\min}$ , where  $\alpha, \gamma, k_{\min}$  and  $k_{\max}$  are parameters of the fit
- $\theta$  independent of centrality (problem is underconstrained)  $\rightarrow \theta$  is a fit parameter

Once the  $P(X|c_b)$  is determined, one obtains:

$$P(c_b | x_1 \leq X \leq x_2) = \frac{\int_{x_1}^{x_2} P(c_b, X) dX}{\int_{x_1}^{x_2} P(X) dX} = \frac{\int_{x_1}^{x_2} P(X|c_b) dX}{\int_{x_1}^{x_2} P(X) dX}$$

and by changing back the variable:  $P(b | x_1 \leq X \leq x_2) = P(b) P(c_b(b) | x_1 \leq X \leq x_2)$

# Reaction centrality

Assessing the impact parameter in experimental data

Physical information is obtained by comparing experimental results and transport model simulations *assuming the same conditions*.

**Impact parameter:** experimentally, it can be only deduced from observables such as multiplicities, transverse energies, flow angle...



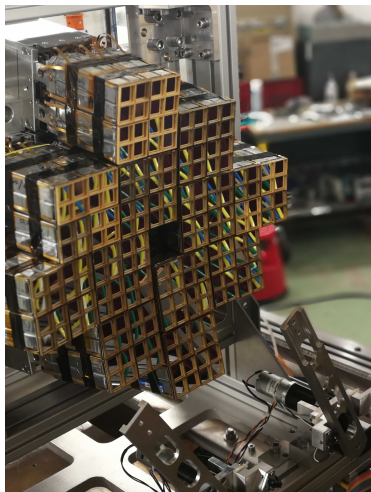
All physics observables are affected by **intrinsic fluctuations** associated with the underlying processes.

Such fluctuations can limit the accuracy in treating centrality and bias the comparisons with simulated data.

L. Li et al., PRC 97,044606 (2018), G. Q. Zhang et al., PRC 84, 034612 (2011)

Different approaches for reaction centrality characterization:

- Sharp cutoff approximation C. Cavata et al., Phys. Rev. C 42, 1760 (1990)
- Machine learning algorithms trained on simulations  
F. Li et al., PRC 104,034608 (2021), F. Haddad et al., PRC 55, 1371 (1997)
- **Model-independent** method to reconstruct impact parameter distributions → includes **fluctuations**  
J. D. Frankland et al., PRC104, 034609 (2021), R. Rogly et al., PRC98, 024902 (2018)



**FAZIA** (*Forward-angle A and Z Identification Array*): optimal ion identification in the Fermi energy domain.

- Result of R&D activities to refine:
  - detector performance
  - digital treatment of signals
- Basic module: **block**, consisting of 16 three stage **telescopes** ( $2 \times 2 \text{ cm}^2$  active area):
  - Si1 300  $\mu\text{m}$  thick
  - Si2 500  $\mu\text{m}$  thick
  - CsI(Tl) 10cm thick
  - + read-out electronics for all telescopes.
- Identification techniques:  $\Delta E - E$  / PSA
  - Charge discrimination tested up to  $Z \sim 55$
  - Mass discrimination up to  $Z \sim 25$  /  $Z \sim 22$

R. Bougault et al., Eur. Phys. J. A 50, 47 (2014)  
S. Valdré et al., NIMA 930, 27 (2019)

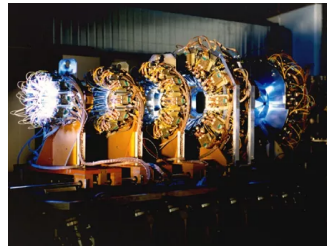
# INDRA

## Main characteristics of the setup

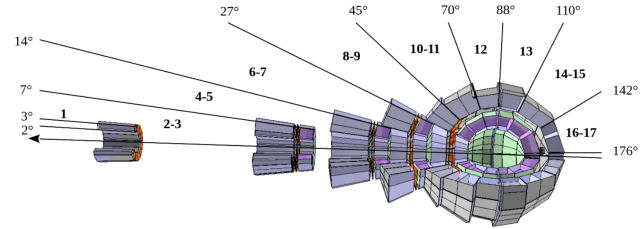
**INDRA** (*Identification de Noyaux et Détection avec Résolutions Accrues*): highly segmented array for detection and identification of charged products of heavy ion collisions at intermediate energies ( $10 < E < 100$  AMeV).

- Original configuration of 17 rings:
  - 1: Phoswich detectors
  - 2-9: Ionisation ch. + Si + CsI(Tl)
  - 10-17: Ionisation ch. + CsI(Tl)
- Charge discrimination up to uranium,  
mass discrimination up to  $Z \sim 4$   
→ Electronics upgrade (2020): now up to  $Z \sim 10$

J. D. Frankland et al., *Nuovo Cim. C* 45, 43 (2022)



- Large solid angle coverage (90%) with high granularity (336 modules)



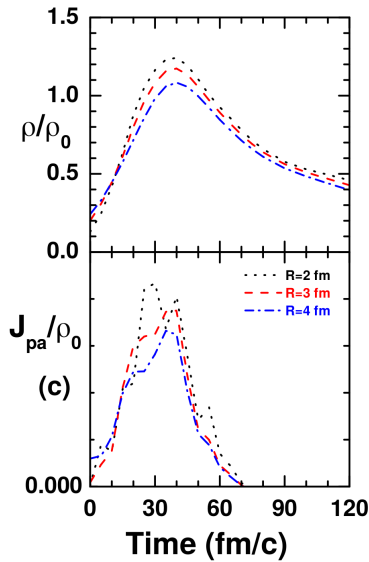
# Sensitive density region

Radius of the examination sphere

The values of baryonic density and isospin current density depend on the radius of the spherical volume used for their evaluation.

- For  $r > 3$  fm the sphere extends beyond the neck region (including empty areas), which reduces both the density and the current density
- For  $r < 3$  fm, the finite number of test particles within the sphere introduces strong statistical fluctuations that affect the current evaluation

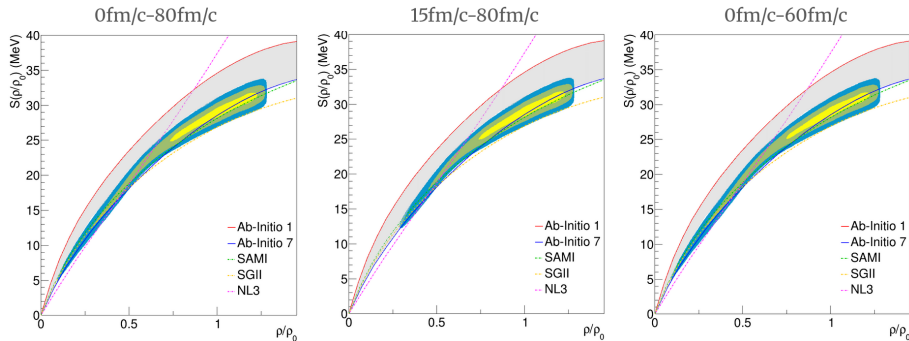
The radius equal to 3 fm has been chosen as the optimal value, balancing these competing effects.



# Constraint on the nuclear EoS

Weighted confidence regions - dependence on  $t$  intervals

The confidence regions slightly depend on the choice of  $b$  and  $t$  intervals for the weight function, but our observations are stable against these arbitrary choices.



e.g., varying the time interval for the weight function evaluation essentially changes the contribution from the low density tail.

# Constraint on the nuclear EoS

Bayesian framework

The proposed procedure corresponds to a **Bayesian parameter estimation**

- of the value of the symmetry energy at different densities  $S_i = S(\rho_i)$
- **not** of the nuclear matter parameters  $S_i \propto \frac{d^i E_{sym}}{d\rho^i}(\rho_0)$  (derivatives at saturation)

The posterior marginalized distribution of  $S_i$  is given by:

$$p(S_i) = \frac{1}{N} \sum_{m=1}^N p(m|\vec{d}) \delta\left(S_i - S_i^{(m)}\right) \quad \text{where} \quad p(m|\vec{d}) = Np^{prior}(m)p(\vec{d}|m)$$

- the set of data  $\vec{d} = \{d_1, \dots, d_K\}$  is the set of ITR data points  $d_j = R(b_j)$
- we consider a gaussian likelihood  $p(\vec{d}|m) \equiv \mathcal{L}_{\vec{d}}(m) = \exp(-\chi_m^2/2)$  with  $\chi_m^2 = \sum_{j=1}^K (d_j - d_j^{(m)})^2 / \sigma_{jm}^2$  and  $\sigma_{jm}^2 = \sigma_{exp,j}^2 + \sigma_{th,jm}^2$
- we take a flat constant prior  $p^{prior}(S(\rho_i))$  for each density  $\rho_i$ , to which we apply the weight function  $p_i^{prior} = w(\rho_i/\rho_0)$ , as a confidence factor on the density axis.  
⇒ globally  $p_i(m|ITR) = w(\rho_i/\rho_0) \exp(-\chi_m^2/2)$